Proceedings World Geothermal Congress 2015
Melbourne, Australia, 19-25 April 2015

Induced Seismicity in Geothermal Reservoirs: Physical Processes and Key Parameters

Emmanuel Gaucher[1], Martin Schoenball[1], Oliver Heidbach[2], Arno Zang[2], Peter Fokker[3], Jan-Diederik van Wees[3,4], and Thomas Kohl[1]

[1]Geothermal Research, AGW, KIT, Adenauerring 20b, 76131 Karlsruhe, Germany

[2]Helmholtz Centre Potsdam, GFZ, Helmholtzstraße 6/7, 14467 Potsdam, Germany

[3]TNO, P.O. Box 80015, NL-3508 TA Utrecht, The Netherlands

[4]Utrecht University, Faculteit van Aardwetenschappen, Boedapestlaan 4, The Netherlands

Corresponding author: emmanuel.gaucher@kit.edu

Keywords: Induced seismicity, Stimulation, EGS, Geomechanics, Numerical modeling

ABSTRACT

In order to reach Europe's 2020 and 2050 targets on greenhouse gas emissions, geothermal resources have to contribute substantially to carbon-free energy needs. Deep geothermal developments, however, are often accompanied by induced seismicity due to stimulation. The induced seismicity can be a threat for the development of future large scale application of deep geothermal power plants. Therefore, understanding the physical processes at the origin of the seismicity induced by forced fluid circulation in geothermal fields is essential, and this paper reviews the current knowledge in connection with field cases.

The driving force of a seismic event is a change of the stress state in the crust. To asses this quantitatively, one needs to know the initial stress state, the spatio-temporal stress changes, the failure criterion, and the rupture dynamics that describes how a seismic event is produced. Several existing geomechanical-numerical models are, in theory, capable of predicting the spatio-temporal changes of the stress state and few of their effects on induced seismicity. They consider coupling between geomechanical, fluid flow, and heat transport processes, with different levels of complexity. The characteristics of the recorded seismicity induced in geothermal fields play a major role to calibrate and to assess the models.

The Soultz-sous-Forêts enhanced geothermal system in France, where thousands of seismic events were induced during stimulations, is an example representative for fields developed in deep crystalline rocks. In such formations, induced seismicity mainly occurs on a network of pre-existing faults and fractures oriented in accordance with the stress field, and shearing on these structures is apparently the dominating failure mechanism. Several physics-based models have been tested on this well-documented field to reproduce the observations. By contrast, the hydraulic fracturing operations carried out in Groß Schönebeck (Germany) geothermal reservoir, which is located in sedimentary formations at a depth similar to Soultz-sous-Forêts, induced very few and weak seismic events. This behavior is consistent with a less seismogenic tensile fracture opening as being the dominant failure mechanism. Interestingly, the few recorded and located seismic events at this site likely occurred on a pre-existing fault.

To characterize a geothermal field with regards to the expected induced seismicity, the following key factors are proposed: natural seismicity at a field scale, stress field, structural fracture/fault characterization, rock type, history of pressure and injection/circulation rates, and past induced seismicity. To mitigate induced seismicity during major hydraulic stimulations, and to prevent large-magnitude event occurrence once injection stopped, early-warning systems and decision support systems are required. To feed these systems, we advocate the application of hybrid methods and the development of fast models. Hybrid methods would combine the best a priori knowledge of the expected behavior of the field underground, inherited from geomechanical-numerical modeling, with a statistical approach based on the real-time observation of the induced seismicity. Fast models would capture the essential physics while minimizing computing time. The quantitative understanding of induced seismicity, however, remains a challenging and complex matter. Only an integration of all current research and development efforts, in the fields of modeling, measuring, monitoring, and matching, will make a chance on success.

1. INTRODUCTION

In order to reach Europe's 2020 and 2050 targets on greenhouse gas emissions, geothermal resources have to contribute substantially to carbon-free energy needs. Geothermal energy is able to provide base load power for electricity and heat generation in many countries around the world, and is predicted to deliver 3-4 percent of the global power need in 2050 (IEA 2011). The vast majority of geothermal energy is currently commercially produced from hydrothermal systems, where hot fluids (water, brine or steam) are extracted from natural high-permeability reservoir rocks. Geothermal energy can be transformed into electrical energy using different conversion technologies and/or directly used as thermal energy in district heating, agriculture, industrial processes, and in spas. In 2010, the worldwide geothermal electric generation capacity was about 10,700 MW and provided about 67.5 TWh per year, less than 1% of the world's energy needs (Bertani 2010).

The use of high-temperature geothermal resources in places such as Iceland and Italy, which benefit from exceptional geological conditions and have a long operational history, is now based on a relatively mature technology for targeting and drilling thermal reservoirs up to 300°C. In magmatic areas, development of deeper reservoirs marked by higher temperatures on the order of 400-700°C (so-called supercritical systems) could significantly increase the share of geothermal energy in the renewable energy portfolio. The key of site-independent geothermal technologies is to use permeable fractures in high-temperature rock so that water and steam circulating into them can rapidly transfer heat to the Earth's surface. Where fractures are not naturally abundant or

permeable, one needs to create new fractures or reactivate existing ones. These enable to extract economical amounts of heat from low-permeability formations (Tester et al. 2006). The so-called enhanced geothermal systems (EGS) require drilling to several kilometers depth to reach adequate temperatures (above 120°C) and involve pumping of fluids at pressure to enhance permeability through the use of hydraulic stimulation or hydraulic fracturing. Because easily accessible hydrothermal systems are becoming increasingly scarce, widespread growth of EGS is anticipated after 2020 and the predicted contribution of EGS to the worldwide geothermal energy production portfolio should be significant for 2050. Research and development should enable EGS to be ready for large scale deployment, both in terms of environmental safety with regards to induced seismicity, and in terms of reducing levelized costs of energy (IEA 2011).

There are a number of environments in which induced seismicity has been observed (Trifu 2002; Trifu 2010). Among these are water-filled dam structures, underground rock excavations, oil and gas production, and underground disposal of waste fluids. Seismicity induced in geothermal fields has been documented for over thirty years in areas such as Indonesia, the Philippines, Japan, North and South America, and New Zealand. In most cases, thousands of seismic events per year are generated during reservoir development and exploitation of a geothermal field, but usually most of them have local magnitude smaller than M_L=3, and are often not felt by people if located in remote areas. An exhaustive description of the seismicity induced and recorded in European geothermal fields or in CO_2 sequestration fields can be found in Evans et al. (2012). Sites in the Rhine Graben structure (Europe) such as Basel (Switzerland, M_L=3.4, 2006), Landau (Germany, M_L=2.7, 2009), and Soultz-sous-Forêts (France, M_L=2.9, 2003) experienced seismicity felt by the population due to development activities of enhanced geothermal systems (EGS). Although the number of events felt by individuals is minor and this seismicity has been short lived, it has attracted public interest due to its proximity to densely populated areas. Besides, at other European sites, the induced seismicity may be of such low magnitude or may occur in such specific geological boundary conditions (e.g. high attenuation of seismic rays due to sediment cover) that it lies below the detection limit of the population.

Induced seismicity is currently perceived by the public as an unsolicited and uncontrollable side effect of geothermal development, especially EGS, and public opinion can be a major show stopper. A good example is the Basel project (Switzerland), where the felt seismic event of M_L=3.4 has led to suspending any further development (Häring et al. 2008). The public perceived induced seismicity as uncontrollable in Basel because the M_L=3.4 event occurred after injection was stopped. As a consequence, project-investors and public administrators are reluctant to support EGS projects.

Examples like these have enhanced the interest in understanding the source of induced seismicity in geothermal applications. Hence, we review the current knowledge of the physical processes used to describe the induced seismicity. Presenting such information in the context of geothermal applications should help to quantify which of the induced underground processes are of importance for the human-induced changes of the physical parameters at depth. Consequently, we first highlight the operational keys (during the development and production phases) which could limit and control the induced seismicity and second to propose directions for further investigations.

2. PHYSICAL PROCESSES

The origin of a seismic event is a variation of in situ stress driving the crust from a stable to an unstable state, up to rock failure. In geothermal applications, the stress changes are due to the numerous effects of fluid circulation within the reservoir. To asses this quantitatively, it is necessary to know a) the stress state of the reservoir under initial conditions, b) the rock failure criterion, its friction characteristics and the associated rupture dynamics, and c) the stress perturbation, in space and time, induced by the anthropogenic underground operations.

2.1 Stress State

Sources of stress on Earth can be classified according to their spatial and temporal scales. Gravity, topography, paleotectonic and tectonic plate motion are typically large-scale stationary sources of stresses. Erosion, sedimentation, regional seismic cycle, aseismic creep can be considered as transient stress sources. Finally, man-made activities such as mining, tunneling, drilling, water impoundment, fluid injection and production would be local sources of stress. For geothermal fields, in most cases only the stress induced by the fluid circulation within the reservoir is considered to change over time and space. The other stress sources are considered in a steady state and are used to quantify the so-called in situ stress state (or natural stress). However, over several ten or more years, this assumption may be too strong depending on the region of interest (e.g. Philippines).

The formal description of the stress acting on a rock body is done with the stress tensor described by three independent orthogonal principal stresses. It is generally assumed that one of the principal stresses corresponds to the vertical stress, S_v, and the other two principal stresses are the minimum and the maximum horizontal stresses, S_h and S_H. Most EGS in Europe are being developed or planned in a strike-slip ($S_H > S_V > S_h$) or normal faulting ($S_V > S_H > S_h$) stress regimes (Cloetingh et al. 2010). The World Stress Map project (Heidbach et al. 2008) compiles information on the contemporary direction of S_H in the crust and stress magnitude compilation is under development (Zang et al. 2012). S_V is usually estimated from the weight of the overburden at the considered depth. S_H and S_h directions may be estimated from borehole breakouts, drilling-induced tensile fractures, hydraulic fractures, or well tests, among other techniques. Several of these techniques also allow determining the amplitude of S_h. However, the quantification of S_H amplitude remains a very challenging task (e.g. Meixner et al. 2014, In Press).

2.2 Rock Failure Criterion and Rupture Dynamics

The rock failure criterion defines the relationship between the material cohesion and the effective stresses acting at the point of failure. Once the critical stress is reached, either pre-existing faults are reactivated or new ones are created. Several rock failure criteria exist (Haimson and Bobet 2012). The Mohr-Coulomb failure criterion (Mohr 1900) is well-known and widely used (). Accordingly, at the point of failure,

$$\tau = c + \mu \cdot \sigma_n \quad (1)$$

where τ, c, μ, σ_n are the shear stress, the cohesion coefficient, the friction coefficient and the effective normal stress, respectively (Figure 1).

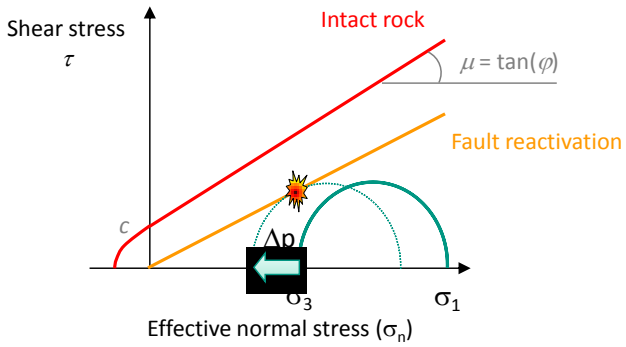

Figure 1: Mohr-Coulomb failure criterion schematic.

The effective stress is the stress felt by the rock grains and is the difference between the in situ stress and the pore pressure. The cohesion is often assumed zero, especially when existing fracture and faults are considered. By referring to Byerlee (1978), the friction coefficient is typically 0.6 – 0.85, depending on the effective normal stress absolute value. These values are suitable for intact rock, however for pre-existing faults, μ could range between 0.3 and 0.6 (e.g. Worum et al. 2004). The Mohr-Coulomb failure criterion, however, only takes into account the extreme principal stresses and proposes linearity of the failure line. Benz and Schwab (2008) compare several criteria and show, for example, that an extended Hoek-Brown criterion, which exhibits a strengthening influence of the intermediate stress and a non-linear dependence on the stress, is a better model. Because they are marked by reduced friction compared to intact rock, already active fractures and faults are most likely loci of seismic activity. Equation 1 shows that failure on a fault is a function of its orientation and of the absolute and relative magnitudes of the effective stresses.

Geomechanical models for earthquakes argue that slip results in a stress drop, which coincides with the removal of asperities reducing friction during faulting. At the end of the faulting process the asperities grow back and re-instate the friction. Scholz (1998) described this using the rate- and state-variable friction law of Dieterich-Ruina (Dieterich 1979; Ruina 1983). The model is consistent with the observation that natural seismicity generally occurs deeper than 3-4 km in the crust.

2.3 Fluid-driven Stress Changes

Prior to geothermal operations, the underground is assumed in a stable steady state. Fluid injection, fluid production and fluid circulation will perturb the in-situ stress field, initially from variation of the pore pressure. Physics-based models are capable of predicting the corresponding stress changes in such an environment. Hence, it is possible to know if the critical stress required to bring the rock to failure is reached. However, the models need to integrate proper coupling of geomechanical, fluid flow, and heat transport processes relevant to induced seismicity in geothermal applications, in addition to realistic parameters, well-chosen boundary conditions, and calibration (Figure 2). The coupled processes are discussed in the following.

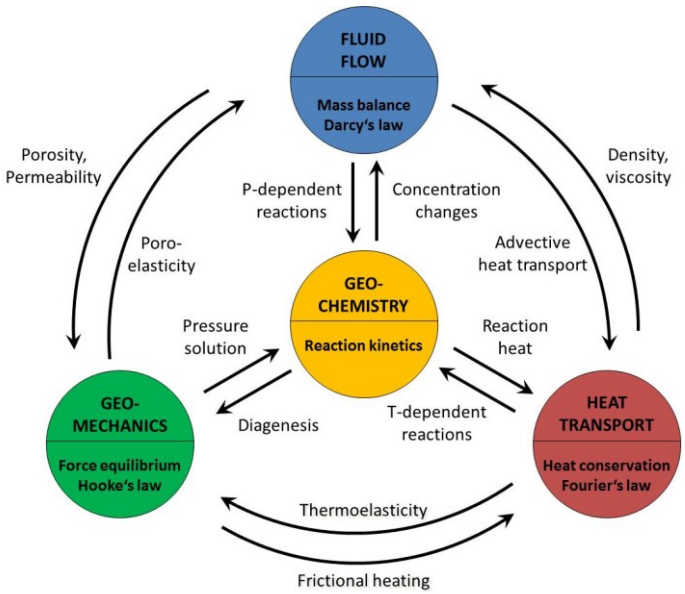

Figure 2: Schematic of the coupled thermo-hydro-mechanical-thermal processes relevant for induced seismicity in geothermal application

Fluid flow is governed by the principle of mass balance and the continuity equation. In geothermal reservoirs, fluid flow may occur in the rock matrix or in faults and fractures. Flow in a porous rock matrix is described by Darcy's law: $v = -K \cdot \nabla p$, where v, K, ∇p

are the Darcy velocity, the hydraulic conductivity and the pressure gradient, respectively. In a fractured medium, the flow rate Q can be expressed by: $Q = -a \cdot k/\eta \cdot \nabla p$, where a, k, η are the fracture aperture, the intrinsic permeability and the dynamic viscosity, respectively. In fractured rock, the permeability $k \approx a^2/12$, resulting in the so-called cubic law, with Q proportional to a^3 (Snow 1965). It represents the common approximation of fluid flow in fractures as flow between parallel plates. The hydraulic field in a fractured medium is thus strongly dependent on the fracture aperture. When pressurizing a fracture, its aperture increases by an elastic response (Willis-Richards et al. 1996), leading to an increase in permeability. The hydraulic response of a reservoir is thus characterized by a rapid increase in pressure even relatively far from the injection source. A consequence is well pressure at equilibrium during constant injection rate, due to continuous permeability creation. Increases of injection rate are followed only by small increases of pressure, as the previous pressurization created additional permeability by elastic opening of the fractures. In nature, fractures have a rough, inhomogeneous aperture which reduces flow, thus decreasing the fracture aperture (Witherspoon et al. 1980). If rough fractures are subject to shear, anisotropy of hydraulic conductivity is introduced (Auradou et al. 2005).

Heat transport occurs in the presence of temperature gradients which exist in geothermal fluid circulation. It is driven by advection, conduction, and radiation, the latter being of no relevance for our application. Advective heat flow is coupled to mass transfer of fluids and thus dominant in rock fractures that serve as a heat exchanger. Conductive heat flow, governed by Fourier's law, is the ruling mechanisms in an impermeable rock matrix. In the course of temperature changes of the rock and the fluid, they tend to expand or contract under temperature changes, causing thermal stresses. As the coefficient of volumetric expansion of water is typically five times larger than that of rock, temperature-induced changes of pore pressure are strongly dependent on the rock permeability (Gens et al. 2007). Furthermore, several material parameters are dependent on temperature. Notably, the fluid viscosity varies by an order of magnitude between 20°C and 100°C.

The geomechanics are governed by force equilibrium and constitutive equations for the different materials. Examples include Hooke's law for a rock matrix with elastic behavior, or other laws for more complex rock behavior like poroelasticity, plasticity, and creep (Jaeger et al. 2007). These laws relate displacement and strain (spatial derivatives of displacement) to stress. The total stress is intrinsically tied to the pore fluid pressure field to form effective stress, which is relevant for the various failure criteria. An increase in pore pressure is only partially transformed into an increase in total stress by the poroelastic effect; therefore the effective stresses are decreased. Increasing/decreasing the fluid content in a continuous porous rock matrix will increase/decrease the pore fluid pressure, but also tend to expand/shrink the volume of the rock matrix, including the pore space, inducing additional stresses. The additional pressures are distributed over time by diffusion, depending on the permeability and the poroelastic stiffness properties of the porous matrix and its constituents. These processes are described by the theory of poroelasticity (Biot 1941; Biot 1962; Rice and Cleary 1976; Wang 2000), in which the pore fluid pressure and stress field are coupled. An analogous coupling exists between temperature and stress field (Zimmerman 2000), it is described by the theory of thermoelasticity (Nowacki 1986). To handle both, they have to be unified to form the theory of thermo-poroelasticity. Analytical solutions exist for a few special cases (Palciauskas and Domenico 1982; McTigue 1986; Kurashige 1989; Wang and Papamichos 1994). For complex problems however, numerical tools have to be used. These tools either solve the complex system of fully coupled differential equations (e.g. Ghassemi et al. 2007; Koh et al. 2011) or rely on a solution scheme that couples sequentially (Rutqvist 2011).

Besides the thermo-poroelastic coupling between fluid flow, heat transfer, and stress in porous rocks, several other coupling mechanisms exist in fractured reservoirs. Tsang (1991) and Rutqvist and Stephansson (2003) give comprehensive reviews of them. The most important mechanisms relevant for geothermal applications are the following. First, massive hydraulic stimulation, production and injection of water under operation conditions cause a massive perturbation of pore fluid pressure and temperature. Both pore fluid pressure increases and temperature decreases can result in rock failure through a lowering of the effective stresses. A temperature decrease diminishes the total stress and the associated effective stress by the thermo-elastic effect which can lead to tensile or shear failure. Second, before a fracture comes to a critical state of stress that induces shearing, the increased pore fluid pressure increases the fracture aperture elastically (Jaeger et al. 2007). Then, the available space for the fluid and the hydraulic conductivity increase considerably (see cubic law), which in turn reduces pore fluid pressure build-up. If, however, pore fluid pressure further increases and a failure criterion is met, shearing occurs that is accompanied by further increases of fracture aperture through dilation. The models the most commonly used to describe the increase of fracture aperture by shearing are those from Barton et al. (1985) and Willis-Richards et al. (1996). Finally, following shearing in a rupture, stresses are redistributed. Close to fracture tips stresses are built-up while along the perimeters stresses are released. Analytical solutions that describe the displacement field induced by static dislocations were derived by Okada (1992) for a homogeneous half-space and later extended for multi-layered elasticity and viscoelasticity by Wang et al (2003; 2006). Hence, aftershock sequences following large earthquakes could be successfully described by modeling of static stress changes (King et al. 1994). The influence of these coseismic static stress changes during reservoir stimulation on induced seismicity is analyzed for example in Schoenball et al. (2012).

Only little progress has been made on the modeling and understanding of geochemical processes coupled to thermo-hydro-mechanical (THM) processes in fractured reservoirs (Figure 2). This is probably related to the little importance attributed to these processes for induced seismicity, at least on a short time scale, but also to the complexity of the topic. Hence, only very few thermo-hydro-mechanical-chemical models (THMC) exist.

2.4 Geomechanical Numerical Models for Induced Seismicity in Geothermal Fields

Only the main characteristics of geomechanical numerical models are discussed here, for more details please see, e.g., Gaucher et al. (In Prep.). The primary results of the numerical models are in most cases the fields of the stress, strain, pore pressure and temperature. To determine them, initial conditions must be stated, such as initial reservoir temperature, pore pressure, saturation degree and in particular in situ stress. The constitutive laws allow modelling the transient stress source due to the man-made perturbations within provided boundary conditions. Finally, the obtained stress field will be checked against a chosen failure criterion to lead to induced seismicity, the secondary result. The resulting catalogues of induced seismicity would be used for probabilistic induced seismic hazard assessment and risk analysis of planned operations. Hence, most of the models do not have the

seismic response as an implemented process but a translation of the primary results into seismicity; in other words, hydraulic and seismic responses are connected in a serial coupling scheme.

To describe the stress field perturbation, the existing models would consider it mainly driven by the rock matrix or an equivalent medium, or by the faults and fractures. The induced seismicity characterization is model-dependent and several of its attributes may typically miss, e.g. seismic event location, energy, stress release. The FRACAS code (Bruel 2007) relies on a fractal distribution of fracture dimensions and, therefore, the resulting magnitude-frequency distribution is controlled by the input parameters. In the model of Kohl and Mégel (2007), pre-existing fractures are partitioned into slip patches. For each time step a shear criterion is evaluated on each slip patch separately and it shears or does not shear independently of any neighboring slip patches. Thus, magnitudes are not obtained by this model, however multiple shearing and the propagation of shearing of one fracture are considered. Upon shearing of a slip patch, the models of Yamashita (1998) and McClure and Horne (2010) calculate associated static stress changes on neighboring slip patches, from analytical solutions by Okada and a displacement discontinuity approach, respectively. This can lead to an avalanche of patch shearing resulting in a large magnitude event when added up. In the model of Baisch et al. (2010), stresses formerly acting on the shearing patch are distributed according to a fixed scheme leading to increase of stress in all neighboring patch elements and possibly triggering shearing of those elements. In the model by Wassing et al. (2014, In Press), the redistribution is calculated through a numerical geomechanical coupling, In Hazzard and Young (2002), rupture is propagated through the interaction of particles. From analysis of moments at the particles, they obtain failure mechanisms and magnitudes.

The models are calibrated from the hydraulic response at the wellbores subject to stimulation (Bruel 2007; Kohl and Mégel 2007; McClure and Horne 2010), and/or from the seismic response of the reservoir (Kohl and Mégel 2007; Rothert and Shapiro 2007). However, on certain observables such as seismicity, fundamentally different physical approaches can be tuned to match the seismic response observed during massive injection operations (e.g. Kohl and Mégel 2007; Rothert and Shapiro 2007). This illustrates the lack of knowledge which prevents from uniquely describing the physical processes occurring in the geothermal reservoir. To prevent from this, calibration on as many parameters as possible is necessary (e.g. pressure and seismicity) (Wassing et al. 2014, In Press).

Once calibrated and validated, the models could forecast the hydraulic behavior and seismic response of a reservoir, and can therefore be used for planning the operations in the reservoir. In EGS for example, the effects on induced seismicity of different stimulation scenarios could be tested, which includes changing injection rate, injection duration, cyclic injection, alternating injection/production cycles (e.g. McClure and Horne 2012; Zang et al. 2013b; Yoon et al. 2014, In Press). Running different simulations with variable input parameters could reproduce the aleatoric uncertainties within the results, and running different models could reproduce the epistemic uncertainties. This could be a procedure for successful implementation of a traffic light system to monitor a stimulation operation and to provide the proper action to react on the actual reservoir response. However, such real-time application is currently limited because numerical models are computationally intensive.

3. CASE STUDIES

In the light of the previous section, we propose physical interpretations of characteristics of the seismicity induced in geothermal fields, and of the main processes which led to it. To illustrate this, we focus on two EGS case studies: Soultz-sous-Forêts (France) and Groß Schönebeck (Germany) which appeared to behave very differently in terms of induced seismicity. However, we also briefly discuss induced seismicity in a hydrothermal system for which no additional fluid is introduced in the reservoir.

3.1 Enhanced Geothermal System, Soultz-sous-Forêts, Upper Rhine Graben, France

3.1.1 Field Context

The development of the Soultz-sous-Forêts (Alsace, France) geothermal field started in 1986 (Genter et al. 2010). It benefits now from a vast amount of field observations in numerous geoscientific domains gathered during the exploration, drilling, stimulation, circulation, production phases. As such, it is a unique database and the lessons learned from this experimental site are applied worldwide. Today, 2.5 MWe gross power can be produced in an ORC cycle and delivered to the French electrical network. Over the development of the EGS, four wells, GPK1, GPK2, GPK3 and GPK4 have been drilled and stimulated to create the heat exchanger. At total depth, the offset between the wells ranges between 450 m and 650 m. The hydraulic exchanger of the current Soultz geothermal field is dominated by a single, large scale fractured zone linking GPK2 and GPK3 in the lower reservoir (Sanjuan et al. 2006).

The Soultz geothermal system practically consists of two major reservoirs: an upper reservoir located at ~3500 m depth, with T=150°C, and a lower reservoir located at ~5000 m depth, with T=200°C (Genter et al. 2010). Both reservoirs reside in the granitic basement which lies below 1400 m of sediment layers. The granitic host rock is however not homogeneous and strongly varies with the older coarse grained pluton sitting above younger fine grained two mica granite. The separation between the two granite types takes place at ~4500 m, also between both reservoirs. From logging measurements, it has been noted that the older granite is strongly altered with mostly illite clay fillings in the fracture and fault zones. In Soultz, the matrix porosity and permeability are respectively 0.5 to 1% and 10^{-5} mD to compare with the fault porosity and permeability below 15% and ~ 1 mD respectively. Hence, fluid circulation in Soultz is expected to be fracture dominated.

Due to the tectonic setting in the Rhine Graben, at the depth of the reservoirs, a normal to strike-slip transitional regime ($S_V \sim S_H$) applies (Cornet et al. 2007; Valley and Evans 2007). The maximum horizontal stress, S_H, is oriented N170°E. At 4100 m depth, S_V=103 MPa, S_H=98-114 MPa and S_h=56 MPa.

In total, eight major hydraulic stimulations were conducted to develop these reservoirs. In average, these stimulations lasted 1 week, about 23,000 m³ of water were injected at maximum 55 L/s for well-head pressures up to 14 MPa. Figure 3 shows the injection schedule for the GPK2 stimulation performed in 2000. Thousands of microseismic events were induced each time, the maximum magnitude event reached M_w=2.9. The induced seismicity was monitored downhole and from surface. The downhole

network, reaching the top of granite (1400 m), was composed of 3 accelerometers and 2 hydrophones. The surface network was composed of more than 15 stations, with three-components and single-components geophones (Cuenot et al. 2008).

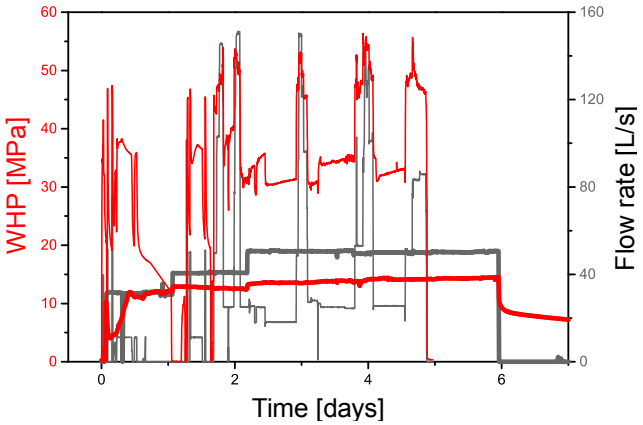

Figure 3: Injection schedules of the Soultz – GPK2 stimulation (thick lines) and of the Groß Schönebeck – GtGrSk4/05 volcanic rock stimulation (thin lines). The grey lines show the flow rate (in L/s) and the red lines the well-head pressure (in MPa).

3.1.2 Key Observations at Soultz

Several major observations about the seismicity induced at Soultz have been made, and interestingly, most of them also applied to other EGS fields.

2D Development of Induced Seismicity

Most of the seismicity induced at Soultz is distributed vertically along a N170°E direction which is consistent with the maximum horizontal stress direction (Charléty et al. 2007; Cuenot et al. 2008; Dorbath et al. 2009) and which is at the origin of the alignment of the four wells along this direction. So, seismicity developed along a 2D network of fractures and faults (or "thick" plane) rather than in a 3D volume. Baisch et al. (2010) highlighted that by statistical collapsing of the locations of the seismic events induced during the 2000 to 2005 deep reservoir stimulations. This almost 2D spatial distribution is also consistent with the fault plane solutions obtained from the focal mechanisms of the seismic events (Cuenot et al. 2006; Dorbath et al. 2010).The focal mechanisms of the largest induced seismic events do not have any significant non-double-couple components which mean that these events are clearly shearing events (Horálek et al. 2010). Distribution of induced seismicity along a single almost horizontal plane was also obvious in the case of Cooper Basin EGS field stimulation of 2003 (Baisch et al. 2006b). When accounting for the rotation of stresses at Cooper Basin (thrust to strike-slip transitional faulting regime $S_H > S_h \sim S_V$ and with S_H being oriented E-W) and Soultz ($S_V \sim S_H > S_h$), the induced seismicity distributions, which are driven by the existing fault system and the stress field, are quite similar. So, the extension of the seismic cloud can be used as a stress field indicator. In the Basel field, seismic events induced during stimulation were also located parallel to the maximum horizontal stress, and the focal mechanisms of most of the strongest ones indicate strike-slip faulting along the maximum horizontal compression stress in the reservoir (Deichmann and Giardini 2009).

Largest Induced Seismicity after Stimulation

As stimulation goes and the flow rate increases, the induced seismicity tends to become of larger magnitude (Dorbath et al. 2009). This behavior was also observed during the GPK3 and GPK4 stimulations, as well as in the Basel EGS field (Häring et al. 2008). Moreover, the induced seismicity does not stop after shut-in despite the subsequent decline of the pressure level at the injection well. Once the injection flow is not sustained any more, no more seismicity is induced in the vicinity of the injection well, but still occurs within the outer rim depicted by the previous seismic activity. At Soultz, in many cases, the largest magnitude events occurred during shut-in phases (Charléty et al. 2007). This happened both for the sudden shut-in of GPK2-2000 stimulation and for the stepwise shut-in carried out in GPK3-2003, suggesting that the shut-in scheme does not play a role in the largest induced seismicity. So, although the seismicity clearly decreases after shut-in, the energy released per event is in average larger.

Kaiser Effect

In our context, the Kaiser effect refers to the observation that seismicity is restricted to areas where fluid overpressure has not been experienced yet in the reservoir and did not generate induced seismicity. This effect is supported by the comparison of seismicity induced by stimulations of the same well and the same reservoir but at different periods of time. This was first noted during the early stimulations performed at Soultz in GPK1 in 1993 (Jones et al. 1995). Charléty et al. (2007) observed that, before injecting at 45 l/s and exceeding the pressure reached during the Nov-2004 stimulation of GPK4, no seismicity was detected during the Feb-2005 stimulation of that well. Similarly, no seismicity should be observed when the stress perturbation declines, and this was observed close to the injection well after shut-in (Parotidis et al. 2004; Baisch et al. 2006a). This was also observed in Basel EGS field (Häring et al. 2008) and again in Cooper Basin EGS field (Baisch et al. 2006b).

Stimulation and Circulation Seismic Response Differences

Such a Kaiser effect may also explain the apparent different behavior between the seismicity induced during stimulation and that induced during circulation. To our knowledge, Soultz is the only EGS field enabling such comparison. Cuenot et al. (2011) describe the seismic behavior during the five circulation tests performed at Soultz, and two principal observations are made. First, the induced event rate seems to increase when the injection well-head pressure also increase and goes above 4.5 or 5 MPa, but it also seems to be correlated to the sudden change of injection flow rates or well shut-in. Second, uncorrelated to the seismicity rate, relatively large events can still be induced during apparently stable circulation conditions. Hence, an M_L=2.3 seismic event was induced in Oct-2005 which is 0.6 point below the largest magnitude event induced at Soultz and four induced seismic events of magnitude above 2 also occurred in 2010. The production scheme was changed for the 2011 circulation test resulting in injection pressures below 2 MPa. This led to a huge drop of the seismic event rate and only five events were recorded during these tests compared to the about 400 induced during the 2010 test. Related to this last point, one can mention that in Landau EGS field (Rhine Graben, Germany, 40 km north from Soultz), the largest induced event (M_L=2.7, 15-Aug-09), which was felt by the population, occurred two years after production started. According to Baumgärtner (2012), no such felt event was induced during stimulation.

Aseismic Behavior of the Stimulated Reservoirs

At Soultz, several observations suggest the occurrence of aseismic slip motions during the stimulations. This behavior was first suspected by Cornet et al. (1997) who analyzed slip motions of several fractures at the wellbore, from ultrasonic imaging logs, before and after the massive 1993 stimulation of GPK1. They noted fracture slip motions up to 4 cm which cannot be explained by one microseismic event but which could be consistent with cumulative slips of microseismic event multiplets (Bourouis and Bernard 2007). The authors concluded that aseismic slip had occurred. Calò et al. (2011) performed a 4-D P-wave tomography of the Soultz lower reservoir during the 2000 stimulation of GPK2. They highlighted significant variations of the velocity field during stationary injection conditions and interpreted them as being caused by effective stress variations linked to fluid diffusion. However, sudden variations were also observed during the changes of injection flow rate, and could not be explained by fluid diffusion. Consequently, the authors considered these changes as resulting from absolute stress variation caused by aseismic motions because the recorded seismicity was not strong enough to explain the stress field variation required.

Soultz is a unique EGS field on which many reservoir and induced seismicity models have been tested (e.g. Gaucher et al. In Prep.). The models have been built from geological and structural information describing the underground and the fractures and faults played an important role besides average rock matrix properties. The knowledge of the stress field and also the rock friction were always a key input parameter.

3.2 Enhanced Geothermal System, Groß Schönebeck, Germany

3.2.1 Field Context

The Groß Schönebeck geothermal site, which is located 40 km north of Germany's capital Berlin, is different from the Soultz site for one major reason. While the reservoir rock at Soultz is of granitic origin, the EGS site at Groß Schönebeck targets the sedimentary Rotliegend formation of the North German Basin.

In December 2000, the former gas exploration well Groß Schönebeck (EGrSk3/90) was reopened and deepened to 4294 m depth to serve as an in-situ geothermal laboratory (Huenges et al. 2006). Nine months after reopening, the bottom hole temperature was 149 °C at 4285 m depth. The reservoir of interest is in the Rotliegend formation and is composed of the Dethlingen sandstones, conglomerates and the underlying andesitic volcanic rocks. The Dethlingen sandstones constitute the principal reservoir. They are well-sorted, middle to fine grained, poorly cemented siliclastic sandstones (Zimmermann et al. 2010) with 8 to 10% porosity and in-situ permeability of 10 – 100 mD. In contrast to the Dethlingen sandstone formation, the permeability of the volcanic rock is rather due to connected fractures (Trautwein and Huenges 2005). The formation pressure was determined from pressure logs after long-term fluid level observations to be about 45 MPa at 4220 m depth. Several stimulation operations were carried out in this well at the reservoir level to enhance water productivity and they are discussed in the next section in parallel with the induced seismicity. To complete the doublet system of this EGS site, the nearby production well GtGrSk4/05 was drilled in 2007 down to the volcanic rocks. At 4236 m TVD, the wells are 470 m apart. In the reservoir section, the hole was deviated and drilled parallel to the minimal horizontal stress direction N288-296°E to increase the thickness of the target layer from 80 m to an apparent thickness of 150 m. The targeted reservoirs are still the volcanic rocks and the overlying Dethlingen sandstones. The stress magnitudes in the Dethlingen sandstone at 4.1 km depth were determined to be S_V=78 - 100 MPa, S_H=98 MPa, and S_h=55 MPa; in the volcanic section, mainly the minimal principal horizontal stress is different and is equal to S_h=72 MPa (Moeck et al. 2009). Hence, the in situ stress magnitudes at Groß Schönebeck, in the sediments, and at Soultz, in the granite, are comparable. Two sets of faults are present in Groß Schönebeck: 1) Major NW-SE trending faults (N130°E) critically stressed and expected to be the main channels for the fluid to move in the reservoir and, 2) a more or less orthogonal, minor joint set oriented NE-SW (N30°E) not critically stressed.

3.2.2 Well Stimulations and Induced Seismicity

In Groß Schönebeck, hydraulic fracturing operations were used to create large and new fractures to gain access to the formation fluids and then to drain the geothermal fluid. The forced fluid injections must therefore decrease the effective minimum principal stress to the tensile strength of the material to develop a mode I failure. This is possible only if the formations are not critically stressed, otherwise new shear zones or preferentially existing faults and fracture may shear first (mode II failure). This latter effect was sought and observed in Soultz for example.

In 2002, two hydraulic fracture treatments were performed to enhance the inflow performance of the former oil exploration well EGrSk3/90, by connecting it to the Rotliegend sandstones (Legarth et al. 2003). The injection rate was 42 l/s at 16 MPa above formation pressure. Unfortunately, no seismic monitoring was done during these operations, so no information on the induced seismicity is available. Yet, it is reasonable to suppose that if seismicity was generated by the operations, it was not strong enough to be felt on the ground. Only the last stimulation treatment of that well was monitored by a network composed of seismic stations deployed at 100 m in dedicated wells. But no microseismic event could be detected (Zimmermann et al. 2010). The monitored

treatment, which was performed in 2003, consisted of a proppant-free water fracturing stimulation at maximum flow rate 40 l/s and leading to the injection of ≈7300 m³ in less than 1 day (Zimmermann et al. 2005).

Seismic monitoring was performed during the first two of the three stimulations performed, in August 2007, in the production well GtGrSk4/05 (Kwiatek et al. 2010). The first treatment took place in the volcanic section at the bottom of the well (Figure 3) and the other two in the sandstone formations. Induced seismic events could only be observed from a three-axis geophone installed in the nearby EGrSk3/90 well, at 3800 m measured depth and about 500 m from the injection point but no seismic event was recorded by the six three-axis geophones operating in shallow wells at 100 m depth, like in the last stimulation of the EGrSk3/90 well. In total, Kwiatek et al. (2010) detected 80 microseismic events, 78 were induced during the 6 days of the volcanic section stimulation. This operation mainly consisted of successive cycles of injection with flow rates ranging from 25 to 150 l/s, the well-head pressure varying mainly above 30 MPa and being smaller than 58.6 MPa. More than 13,000 m³ of fluid were injected in total. Most of the detected events occurred at the early beginning of the injection and after the cycle before the last, five days after stimulation started. However, few events were also recorded after shut-in and during periods of low injection rate. This is most likely because the seismic background noise at the geophone was reduced compared to the high injection rate periods, thus providing highest detection sensitivity. Only 2 microseismic events were induced during the monitored sandstone stimulation, after the initial injection test but before the main gel-proppant treatment, which lasted about one day in cumulative time. Interestingly, the beginning of the volcanic fracturing treatment and that of the lower Dethlingen are very similar in terms of injection rate and well-head pressure and water only was used during these periods; but while the former induced seismicity the latter did not. Unfortunately, the locations of the corresponding microseismic events are not available and therefore it is not possible to know if the events occurred in the volcanic rock or in the sandstones or both and therefore to conclude on possible different seismogenic behaviors between volcanic rock and sandstones. Also, the 2 microseismic events induced during the sediment stimulation may only correspond to reactivation of the zone stimulated during the volcanic rock treatment. Among the 80 recorded events, 29 could be relatively well located using the single three-axis geophone. Seismogram similarities enabled to classify them in three families which led to three clustered distributions in space. Two of them seem to lay on a subvertical structure connecting the volcanic rock and the sandstone layers. Additionally, the seismic event time distribution highlights upward propagation of the seismicity from the volcanic rock into the sandstone. The strike and dip of this planar structure belong to a zone of relatively high-slip tendency, and this seismically active plane is close in orientation and space to a pre-existing fault (F28) mapped earlier from 2D active seismic. So, the majority of the located seismicity, that is the strongest one, most likely occurred on a pre-existing fault re-activated during the stimulation. Finally, we should mention that the estimated moment magnitudes of the located microseismic events range between –1.8 and –1.0. This is very weak compared to other EGS fields (e.g. Evans et al. 2012; Zang et al. 2013a). The total number of identified induced events is also very small but this is likely due to the low sensitivity of the monitoring network with regards to the weak energy seismicity.

Such a low seismogenic behavior was observed in a similar context: the GeneSys project (Orzol et al. 2005; Bischoff et al. 2012). During this project carried out in the region of Hannover (Germany), two different wells were stimulated to increase underground water production from the tight Middle Bunter sandstone formation lying between 3600 and 3900 m depth. Although about 20,000 m³ of water were injected in both wells, with flow rates up to 90 l/s and well-head pressure up to 47 MPa, almost no seismicity was recorded, none was located. Nevertheless, the detection capability of the networks were estimated to be around $M_w = –0.5$.

3.3 Hydrothermal system, Unterhaching, Molasse Basin, Germany

Soultz and Groß Schönebeck consist of EGS in which fluid injections to stimulate the existing fracture network or to generate new fractures lead to an increase of net fluid content in the underground. Accordingly, they can be considered as specific cases of geothermal fields but regarding induced seismicity, such EGS are of main concern because it is well-known that seismicity can be induced, mainly during stimulation, and potentially at a level felt by the population. The hydrothermal systems in which no stimulation is carried out and where no additional fluid is introduced in the reservoir can also induce seismicity while being produced. However, induced seismicity in such systems does not seem to be a major issue for two reasons probably not independent: if seismicity exists, it is hardly ever felt by the population and seismic monitoring of such fields is rare (e.g. Evans et al. 2012).

Unterhaching hydrothermal field is located in the Molasse Basin in Germany. Heat and electricity are generated from a doublet (GT1 and GT2 wells) which produces and re-injects thermal water in the karstic limestone of the Malm (Jurassic) formation between 3000 and 3600 m depth (Wolfgramm et al. 2007). Thermal fluid above 120°C is produced at flow rates up to 120 l/s. In 2008, after heating supply started, two seismic events of magnitude 2.3 and 2.4 which epicenters were located in the vicinity of the geothermal plant were recorded by the regional network (Megies and Wassermann 2014, In Press). In 2010, a local seismic network composed of five surface stations was implemented to record the induced seismicity. Prior to the local network deployment, only 10 events of magnitude between 0.5 and 2.4 were detected; afterwards, 131 events between local magnitude -0.8 and 2.1 were detected with an overall local magnitude of completeness of about -0.2. In total, 90% of the detected seismicity has local magnitude below 1. Absolute locations and relative locations (when possible) highlight that a majority of the epicenters are within a radius of 500-700 m from the injection well and that linear clustering in a NE-SW direction appears, the rest of the seismic events being located in a radius of 1 km but no specific clustering is observable. In depth, the locations range between 4 and 6 km, that is minimum 1.5 km deeper than the injection point; but this may vary (as well as the epicenter locations in a smaller extent) due to the velocity model inaccuracies. Despite these location inaccuracies and the apparent distance between the injection point and the seismic events, it is reasonable to think that several clustered events occurred on a pre-existing NE-SW major trending fault which was also the target of the injection well GT2 (Wolfgramm et al. 2007). Consequently, the question of the impact of the injection on this fault system connected and constituting the geothermal reservoir is relevant, even while the reservoir has high effective transmissivities (10^{-4} m²/s), low overpressure during injection (2.5 MPa (Evans et al. 2012)), and is therefore often seen as free from seismic hazard. As suggested by Megies and Wassermann (2014, In Press), cooling effects may be at the origin of the seismicity.

Interestingly the hydrothermal power plant in Riehen near Basel (Switzerland), despite being only 4 km away from the later abandoned Basel EGS project, did not experience any felt seismicity during its operation for more than 15 years. Here 64°C hot water is produced at a rate of 18 l/s from a 1547 m deep well and re-injected into a 1247 m deep limestone formation. The high subsurface transmissivity allows for operation at very low pressure levels of around 0.7 MPa (Schädle, 2010, internal communication).

4. KEY PARAMETERS

Several lessons have been learned about the seismicity induced in geothermal fields and which were illustrated using the different case studies.

The largest magnitude event induced in geothermal field is not related to one single and simple operational parameter. No direct correlation with either the maximum injection pressure, or the injected volume, or the maximum injection rate exists (Evans et al. 2012).

Seismicity may be induced in EGS as well as non-EGS. In hydrothermal systems, which are often considered as aseismic areas, seismicity can be induced by circulation at magnitudes above 2. Unfortunately, the lack of seismic monitoring in these hydrothermal systems prevents good understanding of the phenomena. The usual high permeability of such systems (and the high fluid circulation rates), and the small overpressures applied to re-inject the fluids, suggest that the fluid flow – geomechanical coupling (Figure 2) is not the principal factor in such a context. Most likely, thermal and geochemical effects play a major role in these systems. Temperature variations will affect hydraulic parameters such as the fluid viscosity but also will deform the rock mass (e.g. thermoelasticity or thermoporoelasticity theories). Besides, the history of the fluid-rock interaction, and the corresponding alteration processes for a given rock type, will affect the fluid path and the behavior of the associated fracture surfaces. For example, weaker clay-filled fractures are likely to shear in a mode different than fresh rough fracture surfaces. Such observation is highlighted, at a large scale, at the San Andreas fault which exhibits both creeping and rupture zones. Interestingly, Schorlemmer and Wiemer (2005) were able to distinguish between these zones using the time and spatial distribution of the b-value of the local seismicity. The high b-values would correspond to creeping mode, and the low b-values to rupture mode.

EGS operations result in much more induced seismicity than other geothermal operations. The injection of net fluid in the subsurface makes a major difference with a fluid circulation. Further, although most of the EGS have been developed in crystalline rocks, seismicity in these formations seems more frequent and stronger than in sedimentary formations, even for similar treatment parameters (e.g. Soultz versus Groß Schönebeck). Hence, soft rocks seem to be less seismogenic, and the crack initiation process is probably one reason. From the available case studies, it is likely that creating a new fracture will induce smaller and weaker seismicity than reactivating existing ones. Hence, rock failure in a mode I, although usually accompanied by dilatant shear failure, is less seismogenic. In the case of Groß Schönebeck, and parallel could be made in the oil and gas industry applications, the largest (still below Mw=-1) induced event apparently occurred on a pre-existing fault (Moeck et al. 2009) which interacted with the fracture treatment. To anticipate on the failure mode, the knowledge of the local stress field, both in direction and amplitude, is fundamental, as is the characterization of the failure conditions. The role of the natural stress field was also highlighted by Van Wees et al (2014, In Press) in the context of seismicity induced by gas production. In low differential effective stress regimes, mode I failure is possible – this is not the case for high differential effective stresses. The existence of natural seismicity around the geothermal field can be used as an indicator of the state of stress of the subsurface as well as for identifying existing faults. In zones with higher natural seismic hazard, shearing is likely to occur at lower hydraulic perturbations and to result in larger magnitudes. This eventually explains why Evans et al. (2012) observe that fields in an area of little natural seismicity may have a lower propensity to produce felt or damaging earthquakes.

The occurrence of a seismic event is controlled by the pre-existing stress field, stress perturbation and fault geometry, but the dynamics of the rupture process is highly dependent on the friction laws governing slip behavior of these faults. So, understanding the dynamic fault friction behavior is crucial to understanding important rupture characteristics such as, for example, the stress drop and size of the seismic event.

The seismic events induced during stimulation of EGS develop within fracture and fault networks which orientations are consistent with the ambient stress field. Induced seismicity development is fracture dominated and the structural fracture characterization is important for estimating the possible expansion of the pressure and flow front in the reservoir. Low fracture densities are likely to focus the pressure front even at larger distances, whereas high fracture densities disperse the front. This effect is also linked to the hydraulic boundary conditions in the reservoir. Open boundaries, that could be large volume fault zones at a graben border, represent a hydraulic drainage system in which little or no pressure increase will occur. These areas are less prone to large magnitude events since they remain hydraulically undisturbed.

The knowledge of the history of pressure and circulating volume (or flow rate) in the reservoir is of major importance. This may explain why in sites like Landau or Soultz, the circulation operations, which followed stimulation operations, show decrease of the induced event rate at low pressure and flow rates, but that outside these conditions, relatively large events can occur instantaneously (Cuenot et al. 2011). Induced seismicity is a time-dependent process. In EGS, the largest magnitude events occurring often after stimulation teach us that seeking for instantaneous time correlation between different operation parameters is certainly wrong. Of course, this time variable makes things a lot more complex. Furthermore, thermal and geochemical effects may be of second order during stimulation but, in the long-term, they are certainly playing a major role which is still difficult to characterize due to the lack of long-term experience.

To summarize, the key factors we propose to use to characterize a geothermal field with regard to the expected induced seismicity are: natural seismicity at a local scale, stress field, structural fracture/fault characterization, rock type, history of pressure and injection/circulation rates, and past induced seismicity. These key parameters may be divided in three families, 1) knowledge of the underground, 2) history or plan of the injection/circulation operations and 3) past and existing seismological observations. While this information will only be partially available, the state of knowledge will typically increase over the development of the

geothermal field. The feasibility phase will bring initial information necessary for drilling the first exploration well which, in turn, will complement and bring many additional key factors. Then, pump tests, stimulations, second well drilling, circulation tests, production will also participate to the knowledge increase.

5. CONCLUSION AND PERSPECTIVES

The EGS operations in Soultz-sous-Forêt and in Groß Schönebeck employed forced fluid injections with similar amount of water, at similar depth, in a similar stress field. However, the cases show drastically different seismic responses, which must be related to differences between the crystalline reservoir and the sedimentary one, and to the differences in the type of performed stimulations. In the hard crystalline rock, shearing on pre-existing fractures was the dominating failure mechanism (mode II failure), inducing many relatively powerful seismic events. In the sedimentary rocks, not critically stressed, mode I fractures were mainly produced, despite the reactivation of an existing fault, in a criticality stressed area, and induced low and weak seismicity. These observations highlight the importance of the failure mechanisms intended for the stimulation and their implication for seismic risk.

At the scale of the geothermal field, the characterization of the stress field, the geological structure, the rock type, the reservoir pressures, the fluid injections and the natural seismicity make first-order physics-based interpretation of induced seismicity possible. This explains why most of the physics-based models of induced seismicity are currently mainly thermo-hydro-mechanical numerical models. Several processes are however still unclear but would certainly play, at least, second-order roles. For example, aseismic creeping of faults, physical processes operating at the contact zone of relaxed and unrelaxed stress areas, and dynamic friction behavior of faults are some topics that need to be investigated further. Efforts should be put into the heat transport description and on the geochemical effects. On a long term perspective, both these processes play a major role, and we suspect them to be first-order processes in hydrothermal systems. Hence, besides the application of existing geomechanical numerical models to stimulations of EGS, use under stationary circulation conditions and in hydrothermal systems is still a perspective.

Physics-based models certainly yield the largest insight into seismic behavior of a reservoir as a function of man-made stress perturbations. So, implementing them in decision support systems during EGS stimulation is particularly interesting to minimize the induced seismic hazard. The effects of different stimulation scenarios could be tested, which represents a strong advantage compared to statistical models. However, such real-time application is currently limited because numerical models are computationally intensive and require the calibration of many parameters acquired during the operation of interest. Two lines of development should therefore be pursued. In the first place, the weight of numerical models during stimulation could be decreased in favor of the so-called statistical approaches which are more suitable to forecast induced seismicity, on a real-time base, from the occurring seismicity, leading to hybrid approach application. In the second place, fast models should be developed that capture the main characteristics of the physics involved but run with dramatically reduced computing times. With both approaches, the parameters and observations gathered during the stimulation period could then be used to calibrate the comprehensive but slower numerical physics-based models. Then, these could play a major role again once the injection stopped and the induced seismicity behavior changed.

The acquisition of reservoir data and seismological observations is of primary importance to improve our understanding of the physics and to quantify the performance, robustness and prediction capabilities of numerical models. Hence, the set-up of geothermal databases is very important to collect the existing knowledge. The quantitative understanding of induced seismicity is a challenging and complex matter. Only an integration of all current efforts in research and development – in the fields of modeling, measuring, monitoring, and matching – will make a chance on success.

ACKNOWLEDGMENTS

The authors would like to thank the EnBW Energie Baden-Württemberg AG, the FP7 project GEISER of the European Commission (grant agreement no. 241321) and the Department of Energy Geothermal Technologies Program (Award Number DE-EE0002756-002) for financial support. The E.E.I.G. "Heat Mining" gave permission to use data from Soultz-sous-Forêts, and C. Dorbath (Strasbourg University) provided the catalogues of the seismicity induced at Soultz-sous-Forêts. The injection schedule data of Groß Schönebeck (Figure 3) were provided by E. Huenges and G. Zimmermann (GFZ). The authors are also grateful to N. Cuenot (E.E.I.G. "Heat Mining"), A. Genter (ES-Geothermie), T. Kölbel (EnBW Baden-Württemberg AG), and G. Zimmermann (GFZ) for fruitful discussions.

REFERENCES

Auradou, H., Drazer, G., Hulin, J. P., and Koplik, J.: Permeability Anisotropy Induced by the Shear Displacement of Rough Fracture Walls, *Water Resour. Res.,* **41**, (2005), W09423.

Baisch, S., Vörös, R., Rothert, E., Stang, H., Jung, R., and Schellschmidt, R.: A Numerical Model for Fluid Injection Induced Seismicity at Soultz-Sous-Forêts, *International Journal of Rock Mechanics and Mining Sciences,* **47**, (2010), 405-413.

Baisch, S., Weidler, R., Vörös, R., and Jung, R.: A Conceptual Model for Post-Injection Seismicity at Soultz-Sous-Forêts, *Geothermal Resources Council Transactions*, (2006a).

Baisch, S., Weidler, R., Voros, R., Wyborn, D., and de Graaf, L.: Induced Seismicity During the Stimulation of a Geothermal Hfr Reservoir in the Cooper Basin, Australia, *Bulletin of the Seismological Society of America,* **96**, (2006b), 2242-2256.

Barton, N., Bandis, S., and Bakhtar, K.: Strength, Deformation and Conductivity Coupling of Rock Joints, *International Journal of Rock Mechanics and Mining Sciences,* **22**, (1985), 121-140.

Baumgärtner, J.: Insheim and Landau: Recent Experiences with Egs Technology in the Urg, *International conference on enhanced geothermal systems (ICEGS)*, (2012).

Benz, T., and Schwab, R.: A Quantitative Comparison of Six Rock Failure Criteria, *International Journal of Rock Mechanics and Mining Sciences,* **45**, (2008), 1176-1186.

Bertani, R.: Geothermal Power Generation in the World 2005-2010 Update Report, *World Geothermal Congress*, 2010.

Biot, M. A.: General Theory of Three Dimensionally Consolidation, *Journal of Applied Physics,* **12**, (1941), 155.

Biot, M. A.: Mechanics of Deformation and Acoustic Propagation in Porous Media, *Journal of Applied Physics,* **33(4)**, (1962), 1482-1498.

Bischoff, M., Keyser, M., Wegler, U., and Bönnemann, C. "Mags-Einzelprojekt 3: Echtzeitauswertung Induzierter Erdbeben Und Gefährdungs-Abschätzung Bei Hydraulischen Stimulationen Geothermischer Reservoire". 2012. BGR. 19 May 2014. <http://www.mags-projekt.de/MAGS/DE/Downloads/MAGS_WS03_EP3.pdf?__blob=publicationFile&v=1>.

Bourouis, S., and Bernard, P.: Evidence for Coupled Seismic and Aseismic Fault Slip During Water Injection in the Geothermal Site of Soultz (France), and Implications for Seismogenic Transients, *Geophysical Journal International,* **169**, (2007), 723-732.

Bruel, D.: Using the Migration of Induced Seismicity as a Constraint for Fractured Hot Dry Rock Reservoir Modeling, *International Journal of Rock Mechanics and Mining Sciences,* **44**, (2007), 1106-1117.

Byerlee, J.: Friction of Rocks, *Pure and Applied Geophysics,* **116**, (1978), 615-626.

Calò, M., Dorbath, C., Cornet, F. H., and Cuenot, N.: Large-Scale Aseismic Motion Identified through 4-D P-Wave Tomography, *Geophysical Journal International,* **186**, (2011), 1295-1314.

Charléty, J., Cuenot, N., Dorbath, L., Dorbath, C., Haessler, H., and Frogneux, M.: Large Earthquakes During Hydraulic Stimulations at the Geothermal Site of Soultz-Sous-Forêts, *International Journal of Rock Mechanics and Mining Sciences,* **44**, (2007), 1091-1105.

Cloetingh, S., van Wees, J. D., Ziegler, P. A., Lenkey, L., Beekman, F., Tesauro, M., Förster, A., Norden, B., Kaban, M., Hardebol, N., Bonté, D., Genter, A., Guillou-Frottier, L., Ter Voorde, M., Sokoutis, D., Willingshofer, E., Cornu, T., and Worum, G.: Lithosphere Tectonics and Thermo-Mechanical Properties: An Integrated Modelling Approach for Enhanced Geothermal Systems Exploration in Europe, *Earth-Science Reviews,* **102**, (2010), 159-206.

Cornet, F. H., Bérard, T., and Bourouis, S.: How Close to Failure Is a Granite Rock Mass at a 5 Km Depth?, *International Journal of Rock Mechanics and Mining Sciences,* **44**, (2007), 47-66.

Cornet, F. H., Helm, J., H, P., and Etchecopar, A.: Seismic and Aseismic Slips Induced by Large-Scale Fluid Injections, *Pageoph.,* **150**, (1997), 563-583.

Cuenot, N., Charléty, J., Dorbath, L., and Haessler, H.: Faulting Mechanisms and Stress Regime at the European Hdr Site of Soultz-Sous-Forêts, France, *Geothermics,* **35**, (2006), 561-575.

Cuenot, N., Dorbath, C., and Dorbath, L.: Analysis of the Microseismicity Induced by Fluid Injections at the Egs Site of Soultz-Sous-Forêts (Alsace, France): Implications for the Characterization of the Geothermal Reservoir Properties, *Pure and Applied Geophysics,* **165**, (2008), 797-828.

Cuenot, N., Frogneux, M., Dorbath, C., and Calò, M.: Induced Microseismic Activity During Recent Circulation Tests at the Egs Site of Soultz-Sous-Forêts (France), *36th Workshop on Geothermal Reservoir Engineering*, 2011.

Deichmann, N., and Giardini, D.: Earthquakes Induced by the Stimulation of an Enhanced Geothermal System Below Basel (Switzerland), *Seismological Research Letters,* **80**, (2009), 784-798.

Dieterich, J. H.: Modeling of Rock Friction 1. Experimental Results and Constitutive Equations, *J. Geophys. Res.,* **84**, (1979), 2161-2168.

Dorbath, L., Cuenot, N., Genter, A., and Frogneux, M.: Seismic Response of the Fractured and Faulted Granite of Soultz-Sous-Forêts (France) to 5 Km Deep Massive Water Injections, *Geophysical Journal International,* **177**, (2009), 653-675.

Dorbath, L., Evans, K., Cuenot, N., Valley, B., Charléty, J., and Frogneux, M.: The Stress Field at Soultz-Sous-Forêts from Focal Mechanisms of Induced Seismic Events: Cases of the Wells Gpk2 and Gpk3, *Comptes Rendus Geoscience,* **342**, (2010), 600-606.

Evans, K. F., Zappone, A., Kraft, T., Deichmann, N., and Moia, F.: A Survey of the Induced Seismic Responses to Fluid Injection in Geothermal and Co2 Reservoirs in Europe, *Geothermics,* **41**, (2012), 30-54.

Gaucher, E., Schoenball, M., Heidbach, O., Zang, A., Fokker, P. A., van Wees, J. D., and Kohl, T.: Induced Seismicity in Geothermal Reservoirs: A Review of Forecasting Approaches, (In Prep.).

Gens, A., Vaunat, J., Garitte, B., and Wileveau, Y.: In Situ Behaviour of a Stiff Layered Clay Subject to Thermal Loading: Observations and Interpretation, *Geotechnique,* **57**, (2007), 207-228.

Genter, A., Evans, K., Cuenot, N., Fritsch, D., and Sanjuan, B.: Contribution of the Exploration of Deep Crystalline Fractured Reservoir of Soultz to the Knowledge of Enhanced Geothermal Systems (Egs), *Comptes Rendus Geoscience,* **342**, (2010), 502-516.

Ghassemi, A., Tarasovs, S., and Cheng, A. H. D.: A 3-D Study of the Effects of Thermomechanical Loads on Fracture Slip in Enhanced Geothermal Reservoirs, *International Journal of Rock Mechanics and Mining Sciences,* **44**, (2007), 1132-1148.

Haimson, B., and Bobet, A.: Introduction to Suggested Methods for Failure Criteria, *Rock Mechanics and Rock Engineering*, (2012), 1-2.

Häring, M. O., Schanz, U., Ladner, F., and Dyer, B. C.: Characterisation of the Basel 1 Enhanced Geothermal System, *Geothermics,* **37**, (2008), 469-495.

Hazzard, J. F., and Young, R. P.: Moment Tensors and Micromechanical Models, *Tectonophysics,* **356**, (2002), 181-197.

Heidbach, O., Tingay, M., Barth, A., Reinecker, J., Kurfeß, D., and Müller, B. "The World Stress Map Database Release 2008". 2008.

Horálek, J., Jechumtálová, Z., Dorbath, L., and Šílený, J.: Source Mechanisms of Micro-Earthquakes Induced in a Fluid Injection Experiment at the Hdr Site Soultz-Sous-Forêts (Alsace) in 2003 and Their Temporal and Spatial Variations, *Geophysical Journal International,* **181**, (2010), 1547-1565.

Huenges, E., Trautwein, U., Legarth, B., and Zimmermann, G.: Fluid Pressure Variation in a Sedimentary Geothermal Reservoir in the North German Basin: Case Study Groß Schönebeck, *Pure and Applied Geophysics,* **163**, (2006), 2141-2152.

IEA. *Technology Roadmap, Geothermal Heat and Power*: International Energy Agency, 2011. Print.

Jaeger, J. C., Cook, N. G. W., and Zimmermann, R.: *Fundamentals of Rock Mechanics, 4th Edition*, *Blackwell publishing*, Oxford, (2007).

Jones, R. H., Beauce, A., Jupe, A., Fabriol, H., and Dyer, B. C.: Imaging Induced Microseismicity During the 1993 Injection Tests at Soultz-Sous-Forêts, France, *World Geothermal Congress*, (1995).

King, G. C. P., Stein, R. S., and Lin, J.: Static Stress Changes and the Triggering of Earthquakes, *Bulletin of the Seismological Society of America,* **84**, (1994), 935-953.

Koh, J., Roshan, H., and Rahman, S. S.: A Numerical Study on the Long Term Thermo-Poroelastic Effects of Cold Water Injection into Naturally Fractured Geothermal Reservoirs, *Computers and Geotechnics,* **38**, (2011), 669-682.

Kohl, T., and Mégel, T.: Predictive Modeling of Reservoir Response to Hydraulic Stimulations at the European Egs Site Soultz-Sous-Forêts, *International Journal of Rock Mechanics and Mining Sciences,* **44**, (2007), 1118-1131.

Kurashige, M.: A Thermoelastic Theory of Fluid-Filled Porous Materials, *International Journal of Solids and Structures,* **25**, (1989), 1039-1052.

Kwiatek, G., Bohnhoff, M., Dresen, G., Schulze, A., Schulte, T., Zimmermann, G., and Huenges, E.: Microseismicity Induced During Fluid-Injection: A Case Study from the Geothermal Site at Groß Schönebeck, North German Basin, *Acta Geophysica,* **58**, (2010), 995-1020.

Legarth, B., Tischner, T., and Huenges, E.: Stimulation Experiments in Sedimentary, Low-Enthalpy Reservoirs for Geothermal Power Generation, Germany, *Geothermics,* **32**, (2003), 487-495.

McClure, M., and Horne, R. N.: Numerical and Analytical Modeling of the Mechanisms of Induced Seismicity During Fluid Injection, *Geothermal Resources Council Transactions*, 2010.

McClure, M. W., and Horne, R. N.: The Effect of Fault Zone Development on Induced Seismicity, *37th Workshop on Geothermal Reservoir Engineering*, 2012, (2011).

McTigue, D. F.: Thermoelastic Response of Fluid-Saturated Porous Rock, *Journal of Geophysical Research-Solid Earth and Planets,* **91**, (1986), 9533-9542.

Megies, T., and Wassermann, J.: Microseismicity Observed at a Non-Pressure-Stimulated Geothermal Power Plant, *Geothermics*, (2014, In Press).

Meixner, J., Gaucher, E., Schill, E., and Kohl, T.: Inferring the in Situ Stress Regime in Deep Sediments: An Example from the Bruchsal Geothermal Site, *Geothermal Energy*, (2014, In Press).

Moeck, I., Kwiatek, G., and Zimmermann, G.: Slip Tendency Analysis, Fault Reactivation Potential and Induced Seismicity in a Deep Geothermal Reservoir, *Journal of Structural Geology,* **31**, (2009), 1174-1182.

Mohr, O.: Welche Umstände Bedingen Die Elastizitätsgrenze Und Den Bruch Eines Materials? [What Are the Conditions for the Elastic Limit and the Fracturing of a Material?], *Zeitschrift des Vereins Deutscher Ingenieure,* **44**, (1900), 1524.

Nowacki, W.: *Thermoelasticity*. 2. ed., rev. and enlarged ed, *Pergamon Pr. [u.a.]*, Oxford [u.a.], (1986).

Okada, Y.: Internal Deformation Due to Shear and Tensile Faults in a Half-Space, *Bulletin of the Seismological Society of America,* **82**, (1992), 1018-1040.

Orzol, J., Jung, R., Jatho, R., Tischner, T., and Kehrer, P.: The Genesys-Project: Extraction of Geothermal Heat from Tight Sediments, *World Geothermal Congress*, 2005.

Palciauskas, V. V., and Domenico, P. A.: Characterization of Drained and Undrained Response of Thermally Loaded Repository Rocks, *Water Resour. Res.,* **18**, (1982), 281-290.

Parotidis, M., Shapiro, S. A., and Rothert, E.: Back Front of Seismicity Induced after Termination of Borehole Fluid Injection, *Geophys. Res. Lett.,* **31**, (2004), L02612.

Rice, J. R., and Cleary, M. P.: Some Basic Stress Diffusion Solutions for Fluid-Saturated Elastic Porous Media with Compressible Constituents, *Rev. Geophys.,* **14**, (1976), 227-241.

Rothert, E., and Shapiro, S. A.: Statistics of Fracture Strength and Fluid-Induced Microseismicity, *J. Geophys. Res.,* **112**, (2007), B04309.

Ruina, A.: Slip Instability and State Variable Friction Laws, *J. Geophys. Res.,* **88**, (1983), 10359-10370.

Rutqvist, J.: Status of the Tough-Flac Simulator and Recent Applications Related to Coupled Fluid Flow and Crustal Deformations, *Computers & Geosciences,* **37**, (2011), 739-750.

Rutqvist, J., and Stephansson, O.: The Role of Hydromechanical Coupling in Fractured Rock Engineering, *Hydrogeology Journal,* **11**, (2003), 7-40.

Sanjuan, B., Pinault, J.-L., Rose, P., Gérard, A., Brach, M., Braibant, G., Crouzet, C., Foucher, J.-C., Gautier, A., and Touzelet, S.: Tracer Testing of the Geothermal Heat Exchanger at Soultz-Sous-Forêts (France) between 2000 and 2005, *Geothermics,* **35**, (2006), 622-653.

Schoenball, M., Baujard, C., Kohl, T., and Dorbath, L.: The Role of Triggering by Static Stress Transfer During Geothermal Reservoir Stimulation, *J. Geophys. Res.,* **117**, (2012), B09307.

Scholz, C. H.: Earthquakes and Friction Laws, *Nature,* **391**, (1998), 37-42.

Schorlemmer, D., and Wiemer, S.: Earth Science: Microseismicity Data Forecast Rupture Area, *Nature,* **434**, (2005), 1086-1086.

Snow, D. T. A Parallel Plate Model of Fractured Permeable Media. Ph.D. Thesis. Berkeley, California, (1965). Print.

Tester, J. W., Anderson, B. J., Batchelor, A. S., Blackwell, D. D., DiPippo, R., Drake, E. M., Garnish, J. D., Livesay, B., Moore, M. C., Nochols, K., Petty, S., Toksöz, M. N., and Veatch, R. W. J.: *The Future of Geothermal Energy: Impact of Enhanced Geothermal Systems (Egs) on the United States in the 21st Century*, *Massachusetts Institute of Technology*, Idaho Falls, (2006).

Trautwein, U., and Huenges, E.: Poroelastic Behaviour of Physical Properties in Rotliegend Sandstones under Uniaxial Strain, *International Journal of Rock Mechanics and Mining Sciences,* **42**, (2005), 924-932.

Trifu, C. I.: Special Issue: Monitoring Induced Seismicity, *Pure and Applied Geophysics,* **167**, (2010).

Trifu, C. I.: Special Issue: The Mechanism of Induced Seismicity, *Pure and Applied Geophysics,* **159**, (2002).

Tsang, C.-F.: Coupled Hydromechanical-Thermochemical Processes in Rock Fractures, *Rev. Geophys.,* **29**, (1991), 537-551.

Valley, B., and Evans, K. F.: Stress State at Soultz-Sous-Forêts to 5 Km Depth from Wellbore Failure and Hydraulic Observations, *32nd Workshop on Geothermal Reservoir Engineering*, 2007.

van Wees, J. D., Buijze, L., Van Thienen-Visser, K., Nepveu, M., Wassing, B., Orlic, B., and Fokker, P. A.: Geomechanics Response and Induced Seismicity During Gas Field Depletion in the Netherlands, *Geothermics*, (2014, In Press).

Wang, H. F.: *Theory of Linear Poroelasticity with Application to Geomechanics and Hydrogeology*, *Princeton University Press*, (2000).

Wang, R. J., Lorenzo-Martin, F., and Roth, F.: Psgrn/Pscmp - a New Code for Calculating Co- and Post-Seismic Deformation, Geoid and Gravity Changes Based on the Viscoelastic-Gravitational Dislocation Theory, *Computers & Geosciences,* **32**, (2006), 527-541.

Wang, R. J., Martín, F. L., and Roth, F.: Computation of Deformation Induced by Earthquakes in a Multi-Layered Elastic Crust--Fortran Programs Edgrn/Edcmp, *Computers & Geosciences,* **29**, (2003), 195-207.

Wang, Y. L., and Papamichos, E.: Conductive Heat-Flow and Thermally-Induced Fluid-Flow around a Well Bore in a Poroelastic Medium, *Water Resources Research,* **30**, (1994), 3375-3384.

Wassing, B. B. T., van Wees, J. D., and Fokker, P. A.: Coupled Continuum Modeling of Fracture Reactivation and Induced Seismicity During Enhanced Geothermal Operations, *Geothermics*, (2014, In Press).

Willis-Richards, J., Watanabe, K., and Takahashi, H.: Progress toward a Stochastic Rock Mechanics Model of Engineered Geothermal Systems, *Journal of Geophysical Research-Solid Earth,* **101**, (1996), 17481-17496.

Witherspoon, P. A., Wang, J. S. Y., Iwai, K., and Gale, J. E.: Validity of Cubic Law for Fluid Flow in a Deformable Rock Fracture, *Water Resour. Res.,* **16**, (1980), 1016-1024.

Wolfgramm, M., Bartels, J., Hoffmann, F., Kittl, G., Lenz, G., Seibt, P., Schulz, R., Thomas, R., and Unger, H. J.: Unterhaching Geothermal Well Doublet: Structural and Hydrodynamic Reservoir Characteristic; Bavaria (Germany), *European Geothermal Congress 2007*, 2007.

Worum, G., van Wees, J.-D., Bada, G., van Balen, R. T., Cloetingh, S., and Pagnier, H.: Slip Tendency Analysis as a Tool to Constrain Fault Reactivation: A Numerical Approach Applied to Three-Dimensional Fault Models in the Roer Valley Rift System (Southeast Netherlands), *J. Geophys. Res.,* **109**, (2004), B02401.

Yamashita, T.: Simulation of Seismicity Due to Fluid Migration in a Fault Zone, *Geophysical Journal International,* **132**, (1998), 674-686.

Yoon, J. S., Zang, A., and Stephansson, O.: Numerical Investigation on Optimized Stimulation of Intact and Naturally Fractured Deep Geothermal Reservoirs Using Hydro-Mechanical Coupled Discrete Particles Joints Model, *Geothermics*, (2014, In Press).

Zang, A., Oye, V., Deichmann, N., Goertz-Allmann, B., Jousset, P., and Gritto, R.: Analysis of Induced Seismicity in Geothermal Reservoirs, an Overview, *Geothermics*, (2013a).

Zang, A., Stephansson, O., Heidbach, O., and Janouschkowetz, S.: World Stress Map Database as a Resource for Rock Mechanics and Rock Engineering, *Geotechnical and Geological Engineering,* **30**, (2012), 625-646.

Zang, A., Yoon, J. S., Stephansson, O., and Heidbach, O.: Fatigue Hydraulic Fracturing by Cyclic Reservoir Treatment Enhances Permeability and Reduces Induced Seismicity, *Geophysical Journal International,* **195**, (2013b), 1282-1287.

Zimmerman, R. W.: Coupling in Poroelasticity and Thermoelasticity, *International Journal of Rock Mechanics and Mining Sciences,* **37**, (2000), 79-87.

Zimmermann, G., Moeck, I., and Blöcher, G.: Cyclic Waterfrac Stimulation to Develop an Enhanced Geothermal System (Egs)-Conceptual Design and Experimental Results, *Geothermics,* **39**, (2010), 59-69.

Zimmermann, G., Reinicke, A., Holl, H.-G., Legarth, B., Saadat, A., and Huenges, E.: Well Test Analysis after Massive Waterfrac Treatments in a Sedimentary Geothermal Reservoir, *World Geothermal Congress*, (2005).